Transient Planetary Waves Simulated by GFDL Spectral General Circulation Models. Part II: Effects of Nonlinear Energy Transfer

Y. HAYASHI AND D. G. GOLDER

Geophysical Fluid Dynamics Laboratory/NOAA, Princeton University, Princeton, NJ 08540

ABSTRACT

In order to study how transient planetary waves in the midlatitude troposphere are maintained, a space–time spectral analysis over a 1-year data set is made of a GFDL spectral general circulation model.

It is found that the kinetic energy (K_n) of both westward and eastward moving ultralong waves with periods less than 20 days is maintained primarily through conversion from wave available-potential energy (A_n).

In particular, A_n of the westward moving ultralong waves is comparable to that of K_n and is maintained primarily through the *wave–wave* transfer of A_n. In contrast, A_n of the eastward moving ultralong waves is larger than K_n and is maintained primarily through the *zonal–wave* transfer of A_n and partly through the wave–wave transfer of A_n. These conclusions also hold in the absence of stationary-transient wave interactions as confirmed by a model with a uniform surface.

1. Introduction

In Part I (Hayashi and Golder, 1983), a space–time spectral analysis has been made of transient planetary waves in the midlatitude troposphere simulated by 9-level, 15-wavenumber spectral Geophysical Fluid Dynamics Laboratory (GFDL) general circulation models with and without mountains. It was found that westward moving ultralong waves are somewhat decreased, while eastward moving ultralong waves are somewhat increased in the absence of mountains in the Northern Hemisphere. This result suggests that transient ultralong waves may not be essentially maintained by stationary-transient wave interactions. It is of interest to study how these waves are maintained in models with and without these interactions.

According to Saltzman's (1970) observational wavenumber spectral analysis (see also Tomatsu, 1979), planetary waves gain kinetic energy and lose available potential energy by wave–wave interaction. However, his conclusion should not be interpreted as describing interactions among *transient* waves, since stationary waves dominate the low wavenumber components. Rather, his result should be interpreted as essentially describing interactions between *stationary* (low wavenumber) and *transient* (middle and high wavenumber) components. This interpretation is consistent with the observational analysis by Lau (1979) who found that the heat transport of transient eddies in the lower troposphere tends to destroy the zonally asymmetric component of the time mean temperature field.

According to the Steinberg *et al.* (1971) analysis (see also Chen, 1982), transient planetary-scale waves lose their available potential energy by wave–wave interactions. However, this conclusion can be erroneous, since their calculation of wave–wave energy transfer of transient waves implicitly includes stationary-transient wave interactions which probably dominate their estimate.[1] According to Hansen and Chen (1982) and Itoh (1983), low wavenumber components can gain available potential energy by wave–wave interaction when they are being amplified.

According to Gambo's (1979) analysis, the wave–wave interaction among planetary waves in the vorticity equation plays an important role in determining the time derivative of the vorticity of ultralong waves. This time derivative, however, can be due to the time change of phase rather than that of amplitude. Thus, it is not clear from his analysis whether the wave–wave interaction plays an important role in the energetics.

Chen *et al.* (1981) compared the linear and nonlinear energy transfer of transient planetary waves simulated by a GLAS general circulation model with those observed by Kao and Lee (1977). Although their results are in agreement, their physical interpretations are in error, since these two studies are based on Kao's (1968) wavenumber–frequency spectral energy equations which are not physically correct,[2] as pointed out by Hayashi (1982a).

---

[1] Steinberg *et al.* (1971) subtracted energy transfer among stationary waves from the total wave–wave energy transfer to obtain this estimate.

[2] Kao's (1968) equation is derived from the imaginary part of a Fourier transformed energy equation which governs the time change of phase.

Hayashi (1980) reformulated the wavenumber (or wavenumber–frequency) spectral energy equations which are physically consistent with Saltzman's (1957) wavenumber energy equations. By use of these equations he compared the nonlinear wavenumber energy transfer spectra of a GFDL 9-level, 30-wavenumber spectral general circulation model (Manabe et al., 1979) with those observed and found reasonable agreement.

In the present paper, a space–time spectral analysis will be made of the energy transfer of simulated transient planetary waves. In order to examine the effect of stationary-transient wave interactions, a model with a uniform surface is also analyzed. In Section 2, wavenumber–frequency energy equations (Hayashi, 1980) are summarized. Section 3 compares the wave energetics of the models with and without a uniform surface. Conclusions and discussions are given in Section 4. Appendix A lists symbols, while Appendix B gives the formulation of nonlinear energy transfer spectra.

2. Wavenumber–frequency energy equations

Wavenumber–frequency energy equations (Hayashi, 1980) are obtained by generalizing the following wavenumber energy equations (see Appendix A for notations).

$$\partial K_n/\partial t = \langle K_m \cdot K_n \rangle + \langle K_0 \cdot K_n \rangle$$
$$- \langle v_n \cdot \nabla \phi_n \rangle + [C_n(u, F_u) + C_n(v, F_v)], \quad (2.1)$$

and

$$\partial A_n/\partial t = \langle A_m \cdot A_n \rangle + \langle A_0 \cdot A_n \rangle$$
$$+ C_n(\alpha, \omega) + (v/C_p)C_n(T, J), \quad (2.2)$$

where C_n denotes wavenumber cospectra and

$$-\langle v_n, \nabla \phi_n \rangle = -C_n(u, \phi_x) - C_n(v, \phi_\theta/r) \quad (2.3a)$$
$$= -C_n(\alpha, \omega) - [\partial C_n(\phi, v)/\partial y$$
$$+ \partial C_n(\phi, \omega)/\partial p]. \quad (2.3b)$$

In the above equations, K_n and A_n are the kinetic and available potential energies for wavenumber n components defined by

$$K_n = [P_n(u) + P_n(v)]/2, \quad (2.4)$$

$$A_n = vP_n(T)/2, \quad (2.5)$$

where P_n denotes wavenumber power spectra and v is defined as

$$v = \frac{R}{p[\kappa \bar{T}^H/p - \partial \bar{T}^H/\partial p]}. \quad (2.6)$$

In (2.1), $\langle K_m \cdot K_n \rangle$ represents the transfer of kinetic energy to the wavenumber n component by inter-

action among all different (m) wavenumber components excluding 0 and n, while $\langle K_0 \cdot K_n \rangle$ represents the transfer of kinetic energy to the wavenumber n component by interaction between zonal flow and the wavenumber n component. Similarly, $\langle A_m \cdot A_n \rangle$ and $\langle A_0 \cdot A_n \rangle$ in (2.2) represent the wave–wave and zonal–wave transfers of available potential energy, respectively. The explicit expressions of these energy transfer spectra are given in Appendix B. It should also be remembered that these spectra represent the transfer of energy, not only among the waves in the latitude–height domain of integration, but also from or to the waves outside this domain.

The wavenumber–frequency energy equations are found by replacing the wavenumber cospectra by wavenumber–frequency cospectra. Wavenumber n and m are understood to be replaced by wavenumber–frequency vectors. The suffix m represents all the wavenumber–frequency vectors except for those associated with 0 and n wavenumbers, while the suffix 0 represents the wavenumber–frequency vector associated with 0 wavenumber. In the present paper, $-\langle v_n \cdot \nabla \phi_n \rangle$ is computed by the direct use of (2.3a).

The wavenumber–frequency spectra have been estimated through the lag correlation method by use of the formulas derived by Hayashi (1971). The methods and applications of space–time spectral analysis are reviewed in Hayashi (1982b). The above energy transfer spectra have been integrated over all the wavenumbers and frequencies and compared with the existing energy diagnostic scheme of GFDL general circulation models to check possible code errors in computing these spectra.

3. Energetics of models

Table 1 shows the wavenumber–frequency spectra over the last year of the model with mountains (see Part I). These spectra are integrated over periods 2–20 days, 29–60°N and 205–980 mb and are classified into three wavenumber ranges of 1–3, 4–9 and 10–15. The high latitudes are excluded, since low wavenumbers may not be interpreted as *ultralong* waves there.

It is seen that the eddy kinetic energy K_n of eastward moving wavenumber 4–9 components is maintained through conversion from the eddy available-potential energy A_n as implied by the positive value of $-\langle v_n \cdot \nabla \phi_n \rangle$. This A_n is in turn maintained through the zonal–wave transfer $\langle A_0 \cdot A_n \rangle$ of available potential energy. These components lose their K_n through the wave–wave transfer $\langle K_m \cdot K_n \rangle$ and zonal–wave transfer $\langle K_0 \cdot K_n \rangle$ of kinetic energy. They lose their A_n through the wave–wave transfer $\langle A_m \cdot A_n \rangle$ of available potential energy.

The wavenumber 1–3 components are associated with a larger westward moving component in the geopotential height, whereas they are associated with a

TABLE 1. Space–time spectra (period $\sim$ 2–20 days) over 1 year's data of the model with mountains integrated over $\sim$29–60°N and $\sim$205–980 mb. Units: geopotential height spectra $z_n'^2$ (10 J s^2 m^{-2}), energy spectra (10^3 J m^{-2}), energy transfer spectra (10^{-3} W m^{-2}).

Wavenumber (n) Direction	Spectra					
	$\sim$1–3		$\sim$4–9		$\sim$10–15	
	West	East	West	East	West	East
$z_n'^2$	60	46	24	80	2	5
K_n	28	39	33	119	10	20
A_n	29	77	28	123	7	13
$\langle K_m \cdot K_n \rangle$	17	−20	1	−167	10	24
$\langle K_0 \cdot K_n \rangle$	7	−5	−1	−12	1	1
$-\langle V_n \cdot \nabla\phi_n \rangle$	43	142	134	464	53	93
$\langle A_m \cdot A_n \rangle$	33	39	48	−12	31	56
$\langle A_0 \cdot A_n \rangle$	9	124	55	623	21	42

TABLE 2. As in Table 1, except for the model with a uniform surface.

Wavenumber (n) Direction	Spectra					
	$\sim$1–3		$\sim$4–9		$\sim$10–15	
	West	East	West	East	West	East
$z_n'^2$	54	48	20	104	2	6
K_n	27	46	24	165	10	27
A_n	25	79	21	129	6	20
$\langle K_m \cdot K_n \rangle$	22	−25	2	−152	12	26
$\langle K_0 \cdot K_n \rangle$	−3	−6	−0	−32	2	2
$-\langle V_n \cdot \nabla\phi_n \rangle$	42	160	92	570	55	148
$\langle A_m \cdot A_n \rangle$	31	37	8	−49	25	50
$\langle A_0 \cdot A_n \rangle$	8	140	58	727	22	78

larger eastward moving component in K_n and A_n. This difference is related to the difference in the meridional and vertical scale of westward and eastward moving components by virtue of the geostrophic and hydrostatic relations. It is shown in Part I that westward moving planetary waves are associated with little vertical tilt and a large meridional wavelength, while the eastward moving planetary waves are associated with some vertical tilt and a small meridional wavelength. It is of importance, however, to note that A_n of the westward moving component is as large as its K_n, in spite of the fact that they are associated with little vertical variation of phase. This result may be due to the effect of vertical shear which affects the vertical variation of amplitude of the external Rossby waves.

It is of interest to note that K_n of the westward moving component is maintained primarily through $-\langle v_n \cdot \nabla\phi_n \rangle$ and to a lesser extent by $\langle K_m \cdot K_n \rangle$. (This conclusion also holds for a period range of 2–7 days.) However, this large $-\langle v_n \cdot \nabla\phi_n \rangle$ does not imply large $\langle A_0 \cdot A_n \rangle$ which turns out to be small compared to the large positive $\langle A_m \cdot A_n \rangle$. Thus it is still reasonable to interpret the westward moving component with relatively small $\langle A_0 \cdot A_n \rangle$ as external waves.

On the other hand, K_n of the eastward moving component is maintained by $-\langle v_n \cdot \nabla\phi_n \rangle$ which is primarily the result of $\langle A_0 \cdot A_n \rangle$ and partly due to $\langle A_m \cdot A_n \rangle$.

The above spectra implicitly include nonlinear energy transfer between transient and quasi-stationary waves. It will be of interest to study whether the above conclusions also hold in the absence of stationary-transient wave interactions. For this purpose, the energetics of a model with a uniform surface are analyzed. This model differs from the model with mountains in that it has no topographical variations in the surface which consists entirely of wet land. Moreover, it has annual mean insolation. This model

has been integrated for approximately 5 years for the purpose of climate variability studies (Held, 1982).

Table 2 is the same as Table 1, except for the last year of the model with a uniform surface. It is confirmed that 1-year mean wave components are negligible against the transient wave components. It is seen that the above conclusions based on Table 1 also hold qualitatively in the absence of stationary-transient wave interactions. It should be noted, in particular, that $\langle A_m \cdot A_n \rangle$ is reduced in the absence of stationary-transient interactions. This implies that the transient waves in Table 1 extract A_n from the stationary waves.

The spectra in Table 2 implicitly include nonlinear energy transfer between transient waves with periods shorter and longer than 20 days. It is of importance to estimate this transfer. Table 3 shows the energy spectra of the model with a uniform surface integrated over wavenumbers 1–15 for periods 2–20 and 20–365 days. It is seen that the short period waves extract A_n from the long period waves which are primarily maintained by $\langle A_0 \cdot A_n \rangle$, and partly by $\langle K_m \cdot K_n \rangle$.

Fig. 1 shows the wavenumber distribution of the

TABLE 3. Space–time spectra (periods $\sim$ 2–20 days and $\sim$20–365 days) of over 1 year's data of the model with a uniform surface integrated over wavenumbers $\sim$ 1–15, $\sim$29–60°N and $\sim$205–980 mb. Units: geopotential height spectra $z_n'^2$ (10 J s^2 m^{-2}), energy spectra (10^3 J m^{-2}), energy transfer spectra (10^{-3} W m^{-2}).

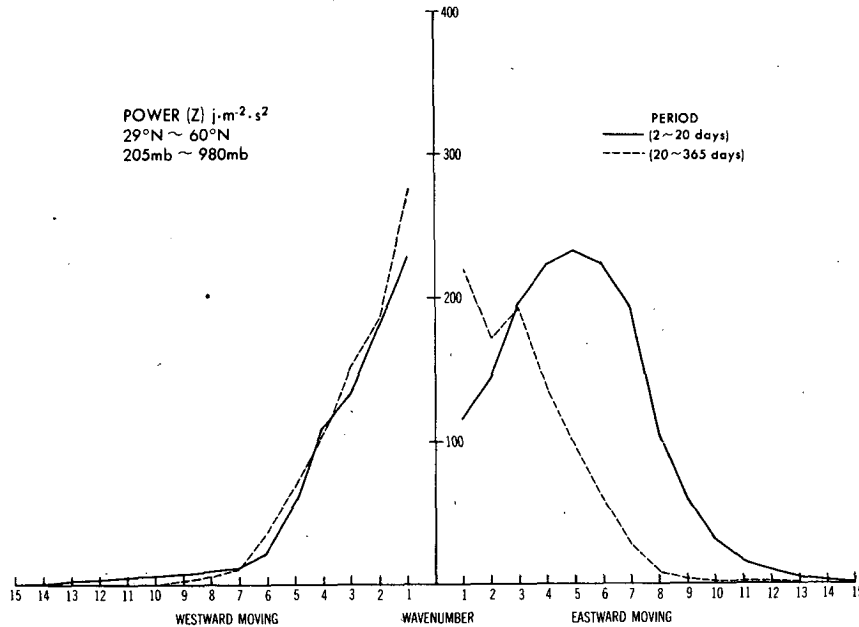| Period (days)	Spectra for $n \sim$ 1–15	
	$\sim$2–20	$\sim$20–365
$z_n'^2$	233	176
K_n	279	143
A_n	275	124
$\langle K_m \cdot K_n \rangle$	−115	42
$\langle K_0 \cdot K_n \rangle$	−38	−36
$-\langle V_n \cdot \nabla\phi_n \rangle$	1067	192
$\langle A_m \cdot A_n \rangle$	102	−91
$\langle A_0 \cdot A_n \rangle$	1033	410

FIG. 1. Wavenumber distribution of the space–time spectra (29–60°N, 205–980 mb) for periods 2–20 days (solid) and 20–365 days (dashed) of geopotential height over one year's data of the model with a uniform surface.

power spectra (period 2–20 and 20–365 days) of geopotential height (29–60°N and 205–980 mb) of the model with a uniform surface. It should be noted that high frequency westward moving ultralong waves are dominated by wavenumber 1, while high frequency eastward moving ultralong waves are dominated by wavenumbers 2 and 3. The low frequency waves are associated with both eastward and westward moving components and are dominated by low wavenumbers. However, the two-dimensional wavenumbers
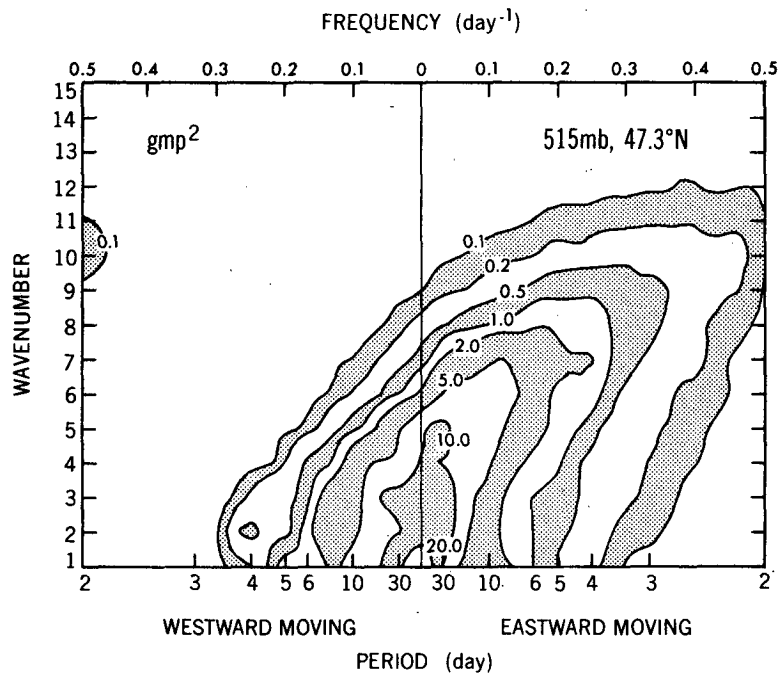
FIG. 2. Wavenumber–frequency distribution of the space–time power spectra (m²) per unit frequency interval (1/365 day⁻¹) of geopotential height at 515 mb, 47.3°N over three years of the model with a uniform surface.

may not be dominated by low two-dimensional wave-numbers.

Fig. 2 shows the wavenumber–frequency spectral distribution of the power spectra of geopotential height at 515 mb, 47.3°N of the model with a uniform surface. Interestingly, this distribution is not very different from that of the models with and without mountains in Part I.

Fig. 3 shows the latitude-frequency distribution of the power spectral density (wavenumber 1) of geopotential height at 515 mb. This distribution is not very different from that of the models with and without mountains in Part I.

4. Conclusions and Remarks

In order to study how transient planetary waves in the midlatitude troposphere are maintained, a space-time spectral analysis is made of GFDL 9-level, 15-wavenumber spectral general circulation models. The conclusions are summarized as follows:

· 1) The westward external ultralong waves with periods 2–20 days are associated with kinetic energy (K_n) and available potential energy (A_n) of comparable magnitude. Their total energy is maintained primarily through the wave–wave transfer of A_n (i.e., $A_m \rightarrow A_n \rightarrow K_n$) and secondarily through wave–wave transfer of K_n.

2) The eastward moving baroclinic ultralong waves with periods 2–20 days are associated with larger A_n than K_n. Their total energy is maintained primarily through the zonal–wave transfer of A_n (i.e., $A_0 \rightarrow A_n \rightarrow K_n$) and partly through the wave–wave transfer of A_n.

3) These conclusions also hold in the absence of stationary-transient wave interactions, as confirmed by a model with a uniform surface.

In summary, K_n of both westward and eastward moving ultralong waves are maintained primarily through conversion from A_n. This A_n is, in turn, maintained primarily through the zonal–wave transfer of A_n except for the westward moving ultralong waves whose A_n is maintained primarily through the wave–wave transfer of A_n. Transient waves with periods 2–20 days, as a whole, extract A_n from quasi-stationary waves. Previously, Manabe et al. (1970), and Gall et al. (1979) also found, by use of grid general circulation models with a uniform surface, that K_n of ultralong waves is maintained primarily through conversion from A_n rather than the nonlinear energy transfer of K_n. However, they did not analyze whether this conversion results from the zonal–wave or wave–wave transfer of A_n. Gall et al. speculated that ultra-long waves are forced by local flux of sensible heat due to modulated cyclone-scale waves. This mechanism can be interpreted essentially as the wave–wave transfer of A_n, since the modulated waves consist of multiple wavenumbers.
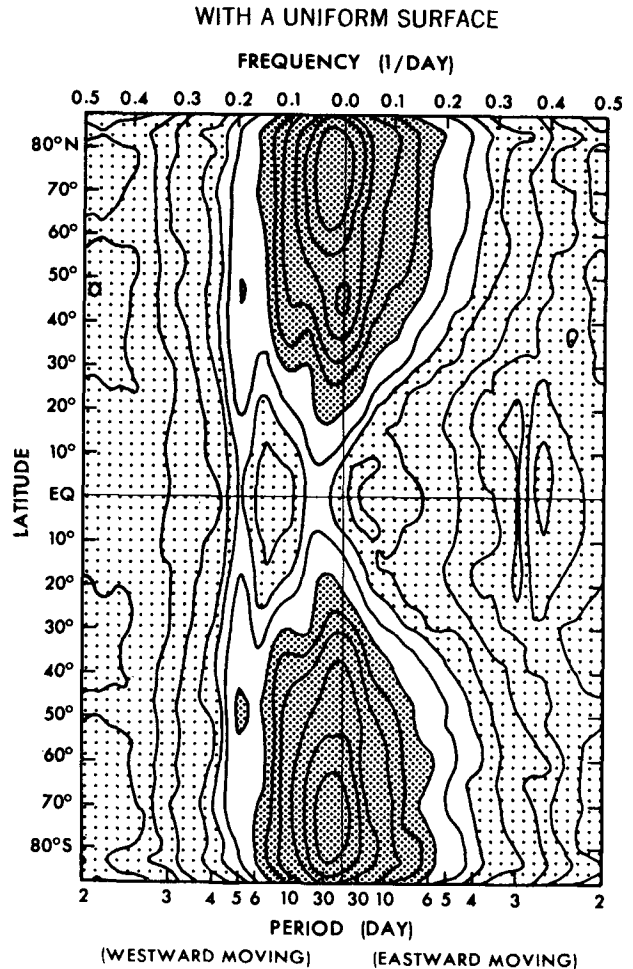
WITH A UNIFORM SURFACE

FREQUENCY (1/DAY)

FIG. 3. Latitude-frequency distribution (wavenumber 1) of the space–time power spectral density (m² day) of geopotential height at 515 mb over three year's data of the model with a uniform surface. Dark shade indicates greater than 500, light shade less than 100. Contour intervals 10, 20, 50, 100, 200, 500, 1000, 2000, 5000, 10000. These values should be divided by 365 to be consistent with the units in Fig. 2.

Conclusion 1) is somewhat surprising, since external waves are commonly thought to involve smaller conversion of energy from A_n to K_n than the wave–wave transfer of K_n. It is of interest to study theoretically the effect of vertical shear on the partition of K_n and A_n. The wave–wave transfer of A_n to the westward moving ultralong waves may be explained by nonlinear resonant interactions between baroclinically unstable and neutral waves as studied by Loesch (1974). These neutral waves can be interpreted as external Rossby waves. Haidvogel and Held (1980) also showed by a numerical two-layer model with a uniform temperature gradient that low wavenumber components are maintained solely through wave–wave interactions.

Conclusion 2) may be, to some extent, explained by the baroclinic instability of realistic zonal mean

states studied by Hartmann (1979) who found that eastward moving ultralong waves with narrow meridional width are associated with larger baroclinic instability (~ 10 days in e-folding time) than those with wide meridional width studied by Green (1960). However, there is the possibility that a slight increase in the growth rate due to wave–wave energy transfer may result in a dramatic increase in the energy level and the zonal-wave transfer.

The present conclusions should be verified observationally by excluding not only stationary waves but also stationary-transient interaction by data analysis as has been demonstrated by Murakami (1978) for tropical kinetic energy spectra. It is also important to study the effect of stationary-transient interaction on the maintenance of stationary waves and the amplifications of quasi-stationary waves. The present analysis describes how transient waves are maintained but should not be interpreted as describing how these waves are occasionally amplified.

APPENDIX A

List of Symbols

Ω	Angular velocity of earth
r	radius of spherical earth 6371 km
λ	longitude
θ	latitude
p	pressure

$$\frac{\partial(\ )}{\partial x} \qquad \frac{\partial(\ )}{r\cos\theta\partial\lambda}$$

$$\frac{\partial(\ )}{\partial y} \qquad \frac{\partial\cos\theta(\ )}{r\cos\theta\partial\theta}$$

m, n	zonal wavenumber ($m \neq 0$, $m \neq n$)
u	eastward velocity
v	northward velocity
ϕ	geopotential
ω	vertical pressure velocity
T	temperature
T^H	global mean temperature
α	specific volume
J	heating rate per unit mass
F	dissipation rate per unit mass

R	gas constant ($=2.8704 \times 10^2$ m^2 s^{-2} K^{-1})
κ	$1 - C_v/C_p$ ($=2/7$)

APPENDIX B

Nonlinear Energy Transfer Spectra

The nonlinear energy transfer spectra can be estimated either by taking a product sum of the Fourier transform of the variables as originally formulated by Saltzman (1957) or more simply by taking a Fourier transform of the product of the variables as proposed by Hayashi (1980). In Hayashi (1980), these terms were derived from equations of motions in the flux form. However, the flux form suffers from a truncation error in the thermodynamics equation, since this form implicitly involves the continuity equation which is not exactly satisfied diagnostically and is multiplied by a large value of temperature. In order to avoid this error the nonlinear energy transfer spectra have been derived from the advective form as given below.

The nonlinear kinetic energy transfer spectrum N_n is written in advective form as

$$N_n = -[C_n(u, uu_x) + C_n(v, uv_x)] - [C_n(u, vu_\theta/r)$$
$$+ C_n(v, vv_\theta/r)] + \tan\theta[C_n(u, uv) - C_n(v, uu)]/r$$
$$- [C_n(u, \omega u_p) + C(v, \omega v_p)], \quad \text{(B1)}$$

where $C_n(a, b)$ denotes wavenumber cospectrum between a and b. This N_n is partitioned into two parts as

$$N_n = \langle K_m \cdot K_n \rangle + \langle K_0 \cdot K_n \rangle, \quad \text{(B2)}$$

where

$$\langle K_m \cdot K_n \rangle = -[C_n(u, u'u'_x) + C_n(v, u'v'_x)]$$
$$- [C_n(u, v'u'_\theta/r) + C_n(v, v'v'_\theta/r)]$$
$$+ \tan\theta[C_n(u, u'v') - C_n(v, u'u')]/r$$
$$- [C_n(u, \omega'u'_p) + C_n(v, \omega'v'_p)] \quad \text{(B3)}$$

and

$$\langle K_0 \cdot K_n \rangle = N_n - \langle K_m \cdot K_n \rangle \quad \text{(B4a)}$$
$$= -[\partial u_0/\partial\theta C_n(u, v) + \partial v_0/\partial\theta C_n(v, v)]/r$$
$$- \tan\theta[u_0 C_n(u, v) - v_0 C_n(u, u)]/r$$
$$- [\partial u_0/\partial p C_n(u, \omega) + \partial v_0/\partial p C_n(v, \omega)]$$
$$- [\partial(v_0 K_n)/\partial y + \partial(\omega_0 K_n)/\partial p]. \quad \text{(B4b)}$$

Here, the suffix 0 denotes the zonal mean, and the prime denotes a deviation from the zonal mean. The subscripts x, θ, p denote derivatives. The x derivative was computed by use of the Fourier series.

The nonlinear available potential energy transfer spectrum N_n is written in advective form as

$$N_n = -\nu C_n(T, uT_x) - \nu C_n(T, vT_\theta/r)$$

$$- \nu C_n(T, \omega T_p) - (\nu\kappa/p)C_n(T, \omega T). \quad (B5)$$

This N_n is partitioned into three parts as

$$N_n = \langle A_m \cdot A_n \rangle + \langle A_0 \cdot A_n \rangle + C_n(\alpha, \omega), \quad (B6)$$

where

$$\langle A_m \cdot A_n \rangle = -\nu C_n(T, u'T'_x) - \nu C_n(T, v'T'_\theta/r)$$

$$- \nu C_n(T, \omega'T'_p) - (\nu\kappa/p)C_n(T, \omega'T') \quad (B7)$$

and

$$\langle A_0 \cdot A_n \rangle = N_n - \langle A_m \cdot A_n \rangle - C_n(\alpha, \omega) \quad (B8a)$$

$$= -\nu\partial T_0/\partial\theta C_n(v, T)/r$$

$$- [\nu(\kappa T_0/p - \partial T_0/\partial p) - R/p]C_n(\omega, T)$$

$$- r^{-1}\partial(v_0 A)/\partial\theta - \partial(\omega_0 A)/\partial p$$

$$+ (\nu^{-1}\partial\nu/\partial p + 2\kappa/p)\omega_0 A. \quad (B8b)$$

The wavenumber–frequency energy equations are obtained by replacing the wavenumber cospectra with wavenumber–frequency cospectra which are estimated through the lag correlation method by use of the formulas derived by Hayashi (1971). In the present paper, wavenumber n and m are understood to be replaced by wavenumber–frequency vectors. The suffix m represents all the wavenumber–frequency vectors except for those associated with 0 and n wavenumbers (not frequencies), while the suffix 0 represents the wavenumber–frequency vector associated with 0 wavenumber and not the zonal time mean.

In the present paper, $\langle K_0 \cdot K_n \rangle$ and $\langle A_0 \cdot A_n \rangle$ are computed by (B4a) and (B8a). These spectra include interactions between the fluctuating zonal flow and waves. When the wavenumber spectra are replaced by wavenumber–frequency spectra, (B4a) and (B8a) no longer coincide with the alternative expressions (B4b) and (B8b), unless the suffix 0 denotes the zonal-time mean.

REFERENCES

Chen, T.-C., 1982: A further study of spectral energetics in the winter atmosphere. *Mon. Wea. Rev.,* **110,** 947–961.
——, H. G. Marshall and J. Shukla, 1981: Spectral analysis and diagnosis of nonlinear interactions of large-scale moving waves at 200 mb in the GLAS general circulation model. *Mon. Wea. Rev.,* **109,** 959–974.
Gall, R., R. Blakeslee and R. C. J. Somerville, 1979: Cyclone-scale forcing of ultralong waves. *J. Atmos. Sci.,* **36,** 1692–1698.

Gambo, K., 1979: A note on the spectral density of vorticity of ultralong waves in middle latitudes at the 500 mb level in the winter season. *J. Meteor. Soc. Japan,* **57,** 373–385.
Green, J. S. A., 1960: A problem in baroclinic stability. *Quart. J. Roy. Meteor. Soc.,* **86,** 237–251.
Haidvogel, D. B., and I. M. Held, 1980; Homogeneous quasi-geostrophic turbulence driven by a uniform temperature gradient. *J. Atmos. Sci.,* **37,** 2644–2660.
Hansen, A. R., and T.-C. Chen, 1982: A spectral energetics analysis of atmospheric blocking. *Mon. Wea. Rev.,* **110,** 1146–1165.
Hartmann, D. L., 1979: Baroclinic instability of realistic zonal mean states to planetary waves. *J. Atmos. Sci.,* **36,** 2336–2349.
Hayashi, Y., 1971: A generalized method of resolving disturbances into progressive and retrogressive waves by space Fourier and time cross-spectral analyses. *J. Meteor. Soc. Japan,* **49,** 125–128.
——, 1980: Estimation of nonlinear energy transfer spectra by the cross spectral method. *J. Atmos. Sci.,* **37,** 299–307.
——, 1982a: Interpretations of space–time spectral energy equations. *J. Atmos. Sci.,* **39,** 685–688.
——, 1982b: Space–time spectral analysis and its applications to atmospheric waves. *J. Meteor. Soc. Japan,* **60,** 156–171.
——, and D. G. Golder, 1983: Transient planetary waves simulated by GFDL spectral general circulation models. Part I: Effects of mountains. *J. Atmos. Sci.,* **40,** 941–950.
Held, I. M., 1982: Stationary and quasi-stationary eddies in the extratropical troposphere: theory. In *Large-scale Dynamical Processes in the Atmosphere,* R. P. Pearce and B. J. Hoskins, Eds., Academic Press, (in press).
Itoh, H., 1983: Observational study on the amplification of planetary waves. Submitted to *J. Meteor. Soc. Japan.*
Kao, S. K., 1968: Governing equations and spectra for atmospheric motion and transports in frequency, wave-number space. *J. Atmos. Sci.,* **25,** 32–38.
——, and H. N. Lee, 1977: The nonlinear interactions and maintenance of the large-scale moving waves in the atmosphere. *J. Atmos. Sci.,* **34,** 471–485.
Lau, N. C., 1979: The observed structure of tropospheric stationary waves and the local balances of vorticity and heat. *J. Atmos. Sci.,* **36,** 996–1016.
Loesch, A. Z., 1974: Resonant interactions between unstable and neutral baroclinic waves: Part I and Part II. *J. Atmos. Sci.,* **31,** 1177–1217.
Manabe, S., J. Smagorinsky, J. L. Holloway, Jr. and H. M. Stone, 1970: Simulated climatology of a general circulation model with a hydrologic cycle. *Mon. Wea. Rev.,* **98,** 175–212.
——, D. G. Hahn and J. L. Holloway, Jr., 1979: Climate simulations with GFDL spectral models of the atmosphere: Effects of truncation. GARP Publ. Ser., No. 22, Vol. 1, 41–94.
Murakami, T., 1978: Winter circulations and wavenumber domain energetics at 200 mb. *J. Meteor. Soc. Japan,* **56,** 215–231.
Saltzman, B., 1957: Equations governing the energetics of the large scales of atmospheric turbulence in the domain of wave number. *J. Meteor.,* **14,** 513–523.
——, 1970: Large-scale atmospheric energetics in the wavenumber domain. *Rev. Geophys. and Space Phys.,* **8,** 289–302.
Steinberg, H. L., A. Wiin-Nielsen and C. H. Yang, 1971: On nonlinear cascades in large-scale atmospheric flow. *J. Geophys. Res.,* **76,** 8629–8640.
Tomatsu, T., 1979: Spectral energetics of the troposphere and lower stratosphere. *Advances in Geophysics,* **21,** Academic Press, 289–405.